Dual Sensory Innervation of Pulmonary Neuroepithelial Bodies

Inge Brouns, Jeroen Van Genechten, Hiroyuki Hayashi, Mariusz Gajda, Toshiaki Gomi, Geoff Burnstock, Jean-Pierre Timmermans, and Dirk Adriaensen

Laboratory of Cell Biology and Histology, University of Antwerp-RUCA, Antwerp, Belgium; Department of Oral Histology, Kanagawa Dental College, Inaoka-cho, Yokosuka, Kanagawa, Japan; Department of Histology, Jagiellonian University, Krakow, Poland; Department of Physical Therapy, Saitama Prefectural University, Koshigaya-City, Japan; and Autonomic Neuroscience Institute, Royal Free and University College Medical School, London, United Kingdom

The characteristics of the different populations of sensory nerve terminals that selectively contact pulmonary neuroepithelial bodies (NEBs) in rat lungs were investigated after chemical denervation with capsaicin and compared with control lungs. Vagal calbindin D28k and $P2X_3$ purinoceptor immunoreactive (IR) afferent nerve terminals contacting NEBs appeared to have their origin in the nodose ganglion. Thick CB/$P2X_3$-IR nerve fibers were seen to be myelinated and to lose their myelin sheaths just before branching and protruding intraepithelially between the NEB cells. This vagal sensory component of the innervation of NEBs was not affected by capsaicin nor expressed capsaicin receptors (vanilloid receptor subtype 1). A second sensory nerve fiber population that selectively innervates pulmonary NEBs in the rat lung consists of thin unmyelinated nonvagal substance P/calcitonin gene-related peptide IR nerve fibers, contacting mainly the basal pole of pulmonary NEBs, and having their origin in dorsal root ganglia. In concordance with vanilloid receptor 1 expression on these nerve terminals, the spinal sensory substance P/calcitionin gene-related peptide-IR component of the innervation of NEBs was depleted by systemic capsaicin treatment. The complex sensory innervation pattern of pulmonary NEBs characterized in the present study strongly suggests that, physiologically, pulmonary NEBs represent a group of intraepithelial receptors that may be able to accommodate various local and central reflex actions, in relation to both chemo- and mechanosensory stimuli.

Primarily based on their sensitivity and responses to a variety of stimuli, and on fiber conduction velocities, single fiber recordings of action potentials have allowed the physiologic classification of different types of airway receptors (for review *see* Ref. 1). In the trachea and bronchi, at least four types of receptors have been postulated, among which are the physiologically well-characterized slowly adapting stretch receptors (SARs), rapidly adapting stretch receptors (RARs), and pulmonary C-fiber receptors, and the more hypothetical sensory receptors in neuroepithelial bodies (NEBs).

(*Received in original form July 15, 2002 and in revised form August 29, 2002*)

Address correspondence to: Dirk Adriaensen, Laboratory of Cell Biology & Histology, University of Antwerp, Groenenborgerlaan 171, B-2020 Antwerp, Belgium. E-mail: dadria@ruca.ua.ac.be

Abbreviations: calbindin D28k, CB; calcitonin gene-related peptide, CGRP; fluorescein isothiocyanate, FITC; immunoreactive/immunoreactivity, IR; myelin basic proteins, MBP; neuroepithelial bodies, NEBs; phosphate-buffered saline, PBS; postnatal day, PD; polyclonal, Pc; protein gene product 9.5, PGP9.5; rapidly adapting stretch receptor, RAR; slowly adapting stretch receptor, SAR; substance P, SP; tyramide signal amplification, TSA; vanilloid receptor subtype 1, VR1.

Am. J. Respir. Cell Mol. Biol. Vol. 28, pp. 275–285, 2003
DOI: 10.1165/rcmb.2002-0117OC
Internet address: www.atsjournals.org

The correlation between the physiologically and morphologically defined lung receptors, however, is far from satisfactory. Although the number of studies dealing with the morphology of the sensory innervation of airways is considerable, the structures of only two types of receptors appear to be recognized: that of the SARs and that of pulmonary NEBs.

Pulmonary NEBs (2) are prime candidates to serve as sensory end organs in the lungs (for reviews *see* Refs. 3, 4). NEBs consist of highly organized clusters of specialized cells with neuroendocrine characteristics, arranged into organoids that are dispersed throughout the epithelium at all levels of the intrapulmonary airways. Ultrastructurally, NEB cells harbor cytoplasmic neurosecretory granules that are known to contain monoamine, peptide, and purine transmitters. In many species, NEBs are preferentially located at or near airway bifurcations, and are as such strategically situated for sensing changes in the airway gas concentration in different parts of the lungs. The use of *in vitro* models of isolated NEBs, combined with electrophysiologic approaches, have provided direct evidence that NEB cells express a membrane-bound O_2 sensor and that they are transducers of hypoxic stimuli (5–7). Moreover, recent cell physiologic data from NEBs in an *in situ* lung slice model (8) and from an immortalized NEB model, the human small cell lung carcinoma cell line H146 (9), have provided direct evidence that a reduced oxygen availability stimulates NEB cells to release bioactive substances (8) via inhibition of O_2-sensitive human TASK-like K^+ channels (9) and the consequent depolarization and calcium-mediated exocytosis. The historical evidence and current state of knowledge of the oxygen-sensing properties of NEB cells have been reviewed recently (10) and have been compared with those of carotid body chemoreceptor cells (11).

The ingrowth of autonomic and sensory fibers converts pulmonary clusters of neuroendocrine cells into NEBs (12). It may be postulated that the innervation is primarily directed toward the integration of chemoreceptive responses. Significantly, NEBs have been estimated to represent a mass of sensory transducing cells and communicating nerves greater in magnitude than the carotid bodies (13), which in many species are widely accepted to serve as the main oxygen sensors for the blood stream.

Previous investigations have provided evidence for two separate populations of sensory nerve fibers that selectively contact pulmonary NEBs in rats (14, 15). Nerve tracing experiments, using the fluorescent anterograde neuronal tracer DiI, revealed that pulmonary NEBs in rats receive an extensive vagal sensory innervation, with origin in the nodose gan-

glion (14). These vagal afferent nerve endings ramify between the NEB cells, and can be labeled by calbindin D28k (CB) and $P2X_3$ purinoreceptor immunoreactivity (IR) (15). They form a nerve fiber population that is clearly different from the sensory calcitonin gene-related peptide (CGRP)-IR innervation (12, 16, 17), which also selectively contacts NEB cells, but does not originate in the nodose ganglion (14).

Although on morphologic grounds the sensory innervation of NEBs is beyond dispute, there are as yet no conclusive experiments establishing their role in the modulation of vagal activity in nodose or jugular ganglia, in axon or local reflexes, or in central nervous reflexes (1). The aim of the present investigation was to fully characterize the functional morphologic characteristics of the dual sensory innervation that selectively contacts pulmonary NEBs. We evaluated the effect of systemic capsaicin treatment (for review *see* Ref. 18) on the vagal and spinal sensory innervation of pulmonary NEBs by quantification of NEBs receiving either CGRP-IR or CB-IR innervation in rats systemically treated with capsaicin and in control rats. Furthermore, the localization of the "capsaicin receptor," vanilloid receptor subtype 1 (VR1), in relation to pulmonary NEBs was evaluated by immunohistochemical staining using antibodies to VR1 and subsequent labeling with antibodies to known markers for rat NEBs. Because an important feature of nervous receptors is their conduction velocity, myelin sheaths were visualized using antibodies raised against myelin basic proteins (MBP) (for review *see* Ref. 19).

Materials and Methods

Animals

Adult Wistar rats of both sexes, and newborn and young animals with their mothers ($n = 34$; Iffa Credo, Brussels, Belgium) were kept in acrylic cages with wood shavings in an acclimatized room (12/12 h light/dark cycle; 22 ± 3°C) and provided with water and food *ad libitum*. National and international principles of laboratory animal care were followed and the experiments were approved by the local ethics committee of the University of Antwerp.

Tissue Processing

All animals (postnatal day 0 [PD0; day of birth] $n = 3$; PD2 $n = 3$; PD4 $n = 3$; PD10 $n = 3$; PD21 $n = 3$; 4–5 wk old, $n = 3$; adults, $n = 8$) were killed using an overdose of sodium pentobarbital (Nembutal; intraperitoneal). Lungs were intratracheally instilled with 4% paraformaldehyde in 0.1 M phosphate buffer, dissected, degassed, and further fixed for 30 min or 2 h. Tissues were rinsed in phosphate-buffered saline (PBS; 0.01 M, pH 7.4), stored overnight in 20% sucrose (in PBS; 4°C) and mounted in Tissue Tek (Sakura Finetek Europe, Zoeterwoude, The Netherlands) on a cryostat chuck by freezing in a CO_2 chamber. Cryostat sections (25–35 μm) were thaw-mounted on poly-L-lysine-coated microscope slides, air dried and processed for immunolabeling.

Immunocytochemical Procedures

All incubations were performed at room temperature in a closed humid container. Characteristics and sources of all primary antisera used are listed in Table 1, those of secondary and tertiary antisera in Table 2. The combinations of primary and secondary antisera used for double immunocytochemical labeling are listed in Table 3. Unless indicated otherwise, all primary and secondary antisera were diluted in PBS containing 10% normal goat serum, 0.1% bovine serum albumin, 0.05% thimerosal, and 0.01% NaN_3 (PBS+). After a final wash, all sections were mounted in Vectashield (Vector Laboratories, Burlingame, CA).

Conventional immunocytochemical double labeling. Cryostat sections were preincubated for 30 min with PBS+ containing 1% Triton X-100, and incubated overnight with a mixture of two primary antibodies raised in different species. After rinsing in PBS, the sections were incubated for 1 h with the appropriate secondary antibodies. The sections labeled with a biotinylated secondary antiserum were additionally incubated for 1 h in fluorochrome-conjugated streptavidin.

Double staining using tyramide signal amplification. To obtain enhanced sensitivity and to allow combination of two antisera raised in the same species, a fluorescein- (NEL701; Perkin-Elmer Life Sciences, Boston, MA) or biotin-conjugated (NEL700; Perkin-Elmer Life Sciences) tyramide signal amplification (TSA) kit was applied (20). In short, endogenous peroxidase activity in cryostat sections of rat lungs was blocked by H_2O_2 (0.4% in 50% methanol in PBS; 10 min), followed by preincubation with PBS+ (containing 1% Triton X-100) and incubation with a primary polyclonal antibody raised in rabbits (*see* Tables 1 and 3). Sections were then consecutively incubated with a biotinylated goat anti-rabbit antibody (diluted 1:500; 1 h) and ExtrAvidin-horseradish peroxidase (diluted 1:1,000 in PBS containing 0.05% thimerosal and 0.1% bovine serum albumin; 1 h). Between subsequent steps the sections were washed three times for 5 min (in 0.05% Tween 20 in PBS). Sections were subjected to TSA-fluorescein (NEL701) or TSA-biotin (NEL-701) tyramide in "amplification solution" (1:100; 10 min), and those subjected to TSA-biotin were subsequently visualized with a fluorochrome-conjugated streptavidin. In many staining procedures used, the sections were subsequently subjected to addi-

TABLE 1
List of primary antisera used for immunocytochemistry

Antigen	Host	Mc/Pc	Source
Calbindin D-28k (CB)	Rabbit	Pc	Swant CB-38, Bellinzona, Switzerland
Calcitonin gene-related peptide (CGRP)	Rabbit	Pc	Affiniti CA1134, Exeter, UK
CGRP	Guinea-Pig	Pc	EuroDiagnostica B-GP 470-1
Capsaicin receptor (VR1)	Rabbit	Pc	Chemicon AB5370, Temecula, CA
Myelin basic protein (MBP)	Rabbit	Pc	DAKO N1546, Carpinteria, CA
$P2X_3$ receptor	Rabbit	Pc	Gift from Roche Bioscience, Palo Alto, CA
Protein gene product 9.5 (PGP9.5)	Mouse	Mc	Biogenesis 7863-2004, Poole, UK
Substance P (SP)	Rabbit	Pc	Sigma S1542, Bornem, Belgium

TABLE 2
List of secondary and tertiary antisera used for immunocytochemistry

Secondary antisera, streptavidin complexes	Source
Biotinylated goat anti-rabbit immunoglobulins (GAR-BIOT)	DAKO E0432
Biotinylated sheep anti-mouse immunoglobulins (SHAM-BIOT)	Amersham Pharmacia, RPN 1001, Roosendaal, The Netherlands
Cy™3-conjugated goat anti-rabbit IgG (GAR-Cy3)	Jackson ImmunoResearch,West Grove, PA; 111-165-144
Cy™3-conjugated streptavidin (Str-Cy3)	Jackson ImmunoResearch 016-160-084
ExtrAvidin-peroxidase	Sigma E2886
Fluorescein (FITC)-conjugated steptavidin (Str-FITC)	Jackson ImmunoResearch 016-090-084
FITC-conjugated Fab Fragment goat anti-rabbit (GAR-Fab-FITC)	Jackson ImmunoResearch 111-097-003
FITC-conjugated goat anti-rabbit IgG (GAR-FITC)	Jackson ImmunoResearch 111-095-144
FITC-conjugated donkey anti-guinea pig (DAGP-FITC)	Jackson ImmunoResearch 706-095-148

tional conventional immunostainings. TSA-enhanced immunostaining for the ATP receptor $P2X_3$ was performed as described previously (15), except that a Cy3-conjugated streptavidin was used to perform visualization.

Control experiments for immunocytochemical procedures. Negative staining controls for all immunocytochemical procedures were performed by substitution of nonimmune sera for the primary or secondary antisera. The general specificity of the primary antibodies for their respective antigens was tested by the providing companies, and the selectivity in rat lung sections in particular was extensively proven using positive and preabsorption controls and was described in our previous publications (15, 20, 21). To check for possible cross-reactivity after consecutive double staining with two rabbit primary antisera, the results of single immunostaining for both substances were evaluated and compared with those from double labeling. Controls for the amplification-based double staining were performed by omission of the primary antiserum of the second incubation. In addition, non-amplified stainings with primary antibodies, using the same concentrations as for the TSA-enhanced reactions were routinely included. To compare TSA-enhanced and conventional methods, conventional immunolabelings were performed using lower dilutions of the primary antisera (*see* controls, Table 3).

Systemic Capsaicin Treatment and Quantitative Analysis

To deplete capsaicin-sensitive primary afferent neurons, adult rats ($n = 4$) were pretreated subcutaneously with a total dose of 125 mg/kg capsaicin (0.4 mmol/kg), 10–14 d before killing. Capsaicin (Fluka, Buchs, Switzerland) was dissolved in PBS (containing 10% ethanol and 10% Tween 80) to give a stock solution of 12.5 g/liter. The total dose of capsaicin was given over 3 d, with 25 mg/kg (0.5 ml) on the first day, and 50 mg/kg (1 ml) on the second and third

TABLE 3
List of used immunocytochemical double staining procedures

Conventional method using two primary antibodies raised in different species

Primary antisera antigen 1	Dilution	Secondary and tertiary reagents	Dilution	Primary antisera antigen 2	Dilution	Secondary and tertiary reagents	Dilution
CGRP	1:500	DAGP-FITC	1:100	CB	1:2,000	GAR-Cy3	1:2,000
CGRP	1:200	GAR-Cy3	1:200	PGP9.5	1:100	SHAM-BIOT	1:100
						STR-FITC	1:100

Tyramide signal amplification (TSA) in combination with conventional labeling (conv.)

Primary antisera antigen 1	Method and visualisation (vis.)	Dilution	Primary antisera antigen 2	Method	Dilution	Secondary reagents	Dilution
SP	TSA-BIOT	1:25,000	CGRP	Conv.	1:500	GAR-Cy3	1:200
	Vis.: Str-FITC	1:2,000					
	Control (conventional)	1:2,000					
VR1	TSA-FITC	1:5,000	CGRP	Conv.	1:500	GAR-Cy3	1:200
	TSA-FITC	1:5,000	CB	Conv.	1:2,000	GAR-Cy3	1:200
	Control (conventional)	1:2,000					
CB	TSA-BIOT	1:25,000	MBP	Conv.	1:1	GAR-Cy3	1:200
	Vis.:Str-FITC	1:2,000					
	Control (conventional)	1:2,000					
$P2X_3$	TSA-BIOT	1:1,600	MBP	Conv.	1:1	GAR-FITC	1:200
	Vis.: Str-Cy3	1:6,000					

days. Control rats ($n = 2$) received equal volumes of vehicle. All injections of capsaicin and its vehicle were performed under ether anesthesia. Rat lungs of capsaicin-treated ($n = 4$), vehicle-injected ($n = 2$), and nontreated controls ($n = 2$) were obtained and processed as described in above-mentioned procedures.

For quantitative analysis of the data, the left lungs of all rats were divided in five segments of ~ 5 mm thickness, perpendicular to the long axis of the lung, the middle piece containing the main bronchi, and frozen on cryostat chucks. The lungs were serially sectioned and 10 random sections, each spaced by at least 4 unused sections to prevent double counts, from each segment were processed for conventional double labeling using antibodies to CGRP and PGP9.5, or to single CB immunocytochemistry. Counts were performed of the total numbers of NEBs (marked by their CGRP/PGP9.5 or CB IR), and of NEBs receiving CGRP- or CB-IR nerve terminals, respectively. Percentages of CGRP or CB-innervated NEBs were compared between capsaicin-treated and control rats. For segment comparison and vehicle-injected and nontreated controls comparison a two-way ANOVA was used. A Student t test was used to compare the group of capsaicin-treated with the control rats. Data are presented as mean percentages ± SD. Differences were considered statistically significant at $P < 0.05$.

Microscopic Analysis

An epifluorescence microscope (Zeiss Axiophot; Carl Zeiss, Zaventem, Belgium) equipped with filters for the visualization of FITC (Zeiss 17; BP 485–20/FT 510/BP 515–565) and Cy3 (Zeiss 14; LP 510-KP 560/FT 580/LP 590) was used to quickly evaluate the results and to perform quantitative analysis of control and capsaicin-treated rats. To obtain detailed images of the individual nerve endings contacting NEBs, confocal laser scanning microscopes (Zeiss LSM 410 and LSM 510) and the attached image reconstruction facilities (Imaris 2.7 software; Bitplane AG, Zurich, Switzerland; Silicon Graphics Indigo 2 workstation) were used. A helium-neon laser (543 nm) and an argon laser (488 nm) were utilized for the excitation of Cy3 and FITC, respectively.

Results

Control Experiments

Substitution of nonimmune sera for the primary or secondary antisera resulted in negative staining controls in all immunocytochemical procedures performed.

After nonamplified indirect immunostaining using the same concentrations of primary antisera (*see* Table 3) as used for TSA-enhanced reactions, no CB, VR1, $P2X_3$ receptor, or SP immunoreactivity (IR) could be detected in rat lungs. In double immunolabelings using TSA-enhanced and subsequent conventional staining, omission of the primary antiserum of the second incubation abolished all immunostaining for the second antigen. No obvious differences could be observed upon comparison of TSA-enhanced and conventional ("control" dilution of primary antisera; *see* Table 3) labeling procedures.

Immunocytochemical Double Staining for CGRP and CB

NEB cells expressing CGRP and CB IR were seen at distinct locations in the epithelium of bronchi, bronchioles (Figure 1), terminal and respiratory bronchioles, and alveolar areas. Typically, CGRP IR was more pronounced in the basal part of the cytoplasm, displaying a granular staining pattern, whereas CB labeling resulted in a more uniform staining of the cytoplasm of NEB cells (Figures 1 and 2). Detailed reconstruction of confocal images showed that all CGRP-IR neuroendocrine cells were also CB-positive (Figures 1 and 2). Some cells at the apical surface of NEBs appeared to show CB IR only (Figure 2).

Apart from being found in neuroendocrine cells, CB and CGRP are expressed in two different sensory nerve fiber populations that selectively contact NEBs. CB IR has been demonstrated to be a marker for the vagal sensory subpopulation (15), whereas CGRP IR most likely labels spinal sensory nerve fibers contacting NEBs.

In the present study, thick, extensively branching CB-IR nerve terminals, which did not show CGRP IR, contacted a subpopulation of NEBs at all levels of the intrapulmonary airways (Figures 1, 2, and 5). Using very sensitive detection methods, the thin varicose CGRP-IR nerve terminals contacting NEBs sometimes revealed a very weak CB IR (Figure 2). Subpopulations of NEBs were contacted by vagal sensory CB-IR nerve terminals alone, by spinal CGRP-IR nerves alone, by both nerve fiber populations, or by neither CB- nor CGRP-IR terminals.

VR1 (Capsaicin Receptor) Immunoreactivity of Sensory Nerve Fibers Selectively Contacting Neuroepithelial Bodies

TSA-enhanced immunocytochemical staining for the capsaicin receptor VR1 and conventional immunolabeling for CGRP showed that in control rats, VR1 is expressed in all CGRP-IR nerve fibers in subepithelial regions and in contact with CGRP-IR NEBs (Figure 4).

Double staining for VR1 and CB showed that a subpopulation of the CB-IR NEBs is contacted by VR1-IR nerve terminals (Figure 5). Reconstructions of optical sections obtained by confocal microscopy revealed that the VR1-IR nerve terminals were not CB-IR (Figure 5), although the CB-IR nerve fibers could be seen to run in very close proximity to VR1-IR fibers (Figure 5).

Detailed Spatial Relationship of Spinal Sensory Nerve Terminals and Pulmonary Neuroepithelial Bodies

In lung sections double-immunostained for SP and CGRP, or for VR1 and CGRP, CGRP-IR NEB cells found in the epithelium at all levels of the intrapulmonary airways (Figures 3 and 4) never showed SP (Figure 3) or VR1 IR (Figure 4). Thin varicose SP/CGRP-IR or VR1/CGRP-IR nerve fibers were found to be associated with a subpopulation of NEBs (Figures 3 and 4). Reconstruction of optical sections obtained by confocal microscopy showed that a number of NEBs were contacted by thin varicose branching VR1/CGRP- or SP/CGRP-IR nerve endings at their basal side only, thereby often forming an extensive network (Figures 3 and 4). Two-dimensional reconstructions of confocal optical sections in three perpendicular planes clearly showed that the SP/CGRP-IR nerve endings mainly surround the base of the CGRP-IR NEB cells, but generally do not protrude between the cells (Figure 3).

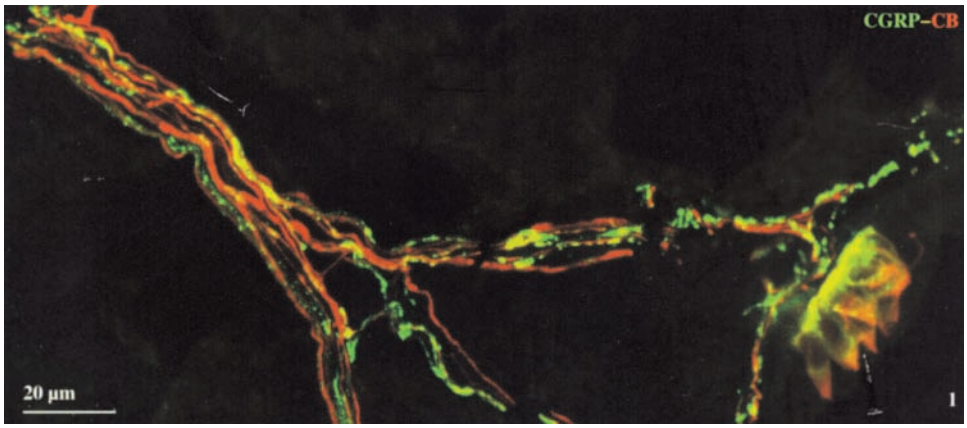

Figure 1. Overview of an NEB located in the epithelium of a bronchiole of a 10-d-old rat double stained for CGRP (*green FITC fluorescence*) and CB (*red Cy3 fluorescence*). CGRP/CB-IR NEB cells are contacted by a nerve bundle composed of thick CB-IR nerve fibers and varicose CGRP-IR nerve terminals. Note that in the NEB cells CGRP labeling is strongest at the basal side, whereas CB labeling appears to be more uniform throughout the cells. Maximum intensity projection of 19 optical sections (1.3-µm interval).

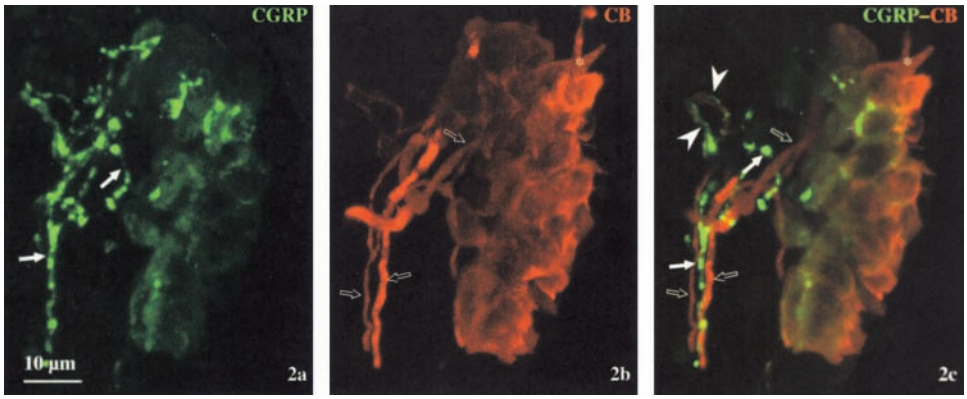

Figure 2. Maximum intensity projection of 34 confocal optical sections (1-µm interval) of an NEB in a bronchus of a 10-d-old rat. (*a*) Green channel showing a granular pattern of CGRP IR in NEB cells that are contacted by CGRP-IR nerve fibers (*arrows*). (*b*) Red channel showing a bundle of CB-IR nerve fibers (*open arrows*) that contact the CB-IR NEB cells. Apparently, some of the CB-IR cells (*asterisk*) do not express CGRP. (*c*) Combination of both channels reveals that CGRP and CB are located in separate nerve fiber populations. Note that some of the CGRP-IR nerve fibers show very weak CB IR (*arrowheads*).

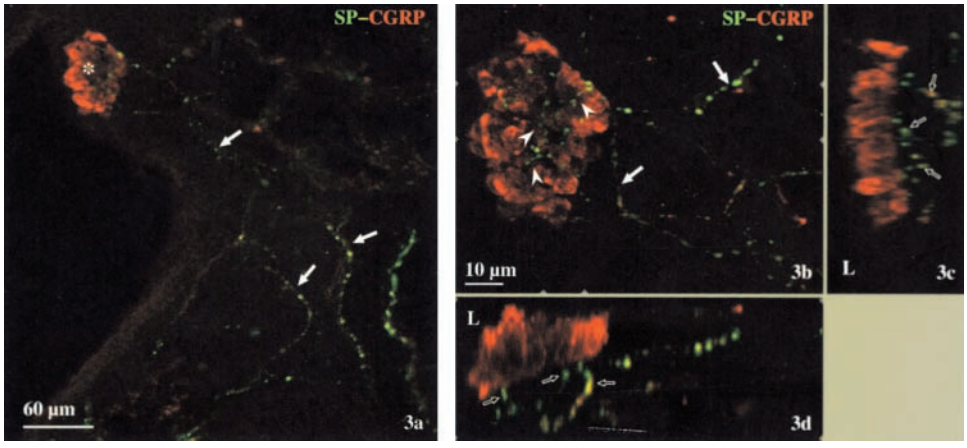

Figure 3. TSA-enhanced immunocytochemical staining for SP (*green FITC fluorescence*) and sequential conventional staining for CGRP (*red Cy3 fluorescence*) of an NEB in an intrapulmonary bronchus of a 5-wk-old rat. (*a*) Low-magnification overview showing an extensive network of SP/CGRP-IR nerve fibers. SP/CGRP-IR nerves are seen to make contact with a CGRP-IR NEB (*asterisk*). Single optical section. (*b–d*) Confocal reconstructions in three perpendicular planes. (*b*) High magnification of the NEB in *a*. Maximum intensity projection of 27 optical sections (2-µm interval) showing an extensive network of SP/CGRP-IR nerve fibers (*arrows*) in contact with the CGRP-IR NEB (*arrowheads*). (*c–d*) Electronic cross-sections, the thickness of which is indicated by *small triangles* at the *bottom margin* of *b* (for *c*) and at the *right margin* of *b* (for *d*), perpendicular to the airway surface of the NEB, demonstrate that the SP/CGRP-IR nerves contact the NEB only at its basal pole (*open arrows*). SP/CGRP-IR nerve fibers were never seen to protrude between the neuroendocrine cells, although the reconstructed tangential view in *b* may erroneously give that impression (L, bronchial lumen).

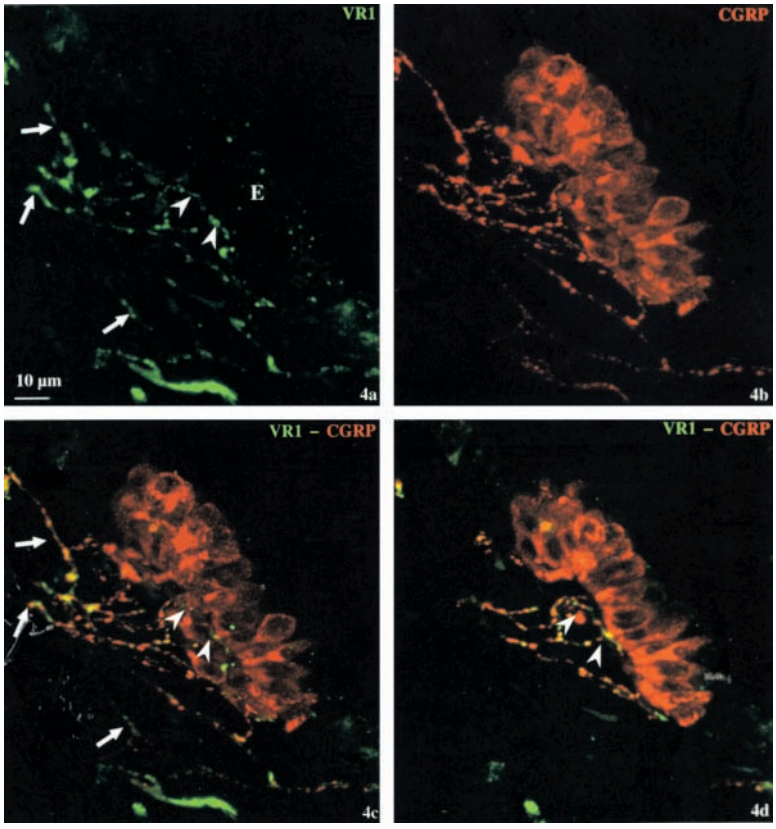

Figure 4. TSA-enhanced immunocytochemical staining for VR1 (green FITC fluorescence) combined with conventional immunostaining for CGRP, as a marker for the spinal sensory subpopulation (red Cy-3 fluorescence) of nerve terminals contacting a bronchiolar NEB in a 10-d-old rat. (*a–c*) Maximum intensity projection of 30 optical sections (1-μm interval) (*a*) *Green* channel showing abundant VR1-IR nerve fibers in the lamina propria (*arrows*) that contact the base of the bronchiolar epithelium (*arrowheads*). No VR1 IR is seen in epithelial cells (E). (*b*) *Red* channel showing a CGRP-IR NEB contacted by extensively branching CGRP-IR nerve endings. (*c*) Combination of both channels clearly shows that the CGRP-containing nerve fibers also express VR1 (*arrows* and *arrowheads*), the yellow fluorescence being indicative of co-localization. CGRP-IR NEB cells obviously do not show VR1 IR. (*d*) Reconstruction of five optical sections of the same stack as in *c* clearly demonstrating the basally restricted localization (*arrowheads*) of VR1/CGRP-IR nerve endings.

Capsaicin Treatment Affects CGRP-IR but Not CB-IR Nerves in Contact with NEBs

Double immunocytochemical staining for CGRP and PGP9.5 (Figure 8a) revealed that in nontreated and vehicle-injected healthy adult rat lungs, ~ 50% of the counted NEBs were selectively contacted by CGRP-IR nerve terminals. After systemic capsaicin treatment, the number of NEBs receiving CGRP-IR terminals significantly decreased to ~ 5%. In control as well as in capsaicin-treated rats, all pulmonary NEB cells showed complete colocalization of PGP9.5 and CGRP IR.

Immunocytochemical staining for CB showed that ~ 40% of the counted NEBs in nontreated healthy rat lungs were selectively contacted by CB-IR nerve terminals, a percentage that was not altered significantly after capsaicin treatment (Figure 8b).

Vagal Sensory Nerve Fibers that Originate in Nodose Ganglia and Selectively Contact Pulmonary Neuroepithelial Bodies Are Myelinated

At PD0, MBP IR can be seen in myelin sheaths of some nerve fibers in large nerve bundles (N. vagus, N. phrenicus). From PD2 onwards, MBP IR can be localized intrapulmonarily in myelin sheaths of nerve fibers located in large bundles, as well as in apparently solitary nerve fibers. Myelinated vagal sensory nerve fibers contacting NEBs, as

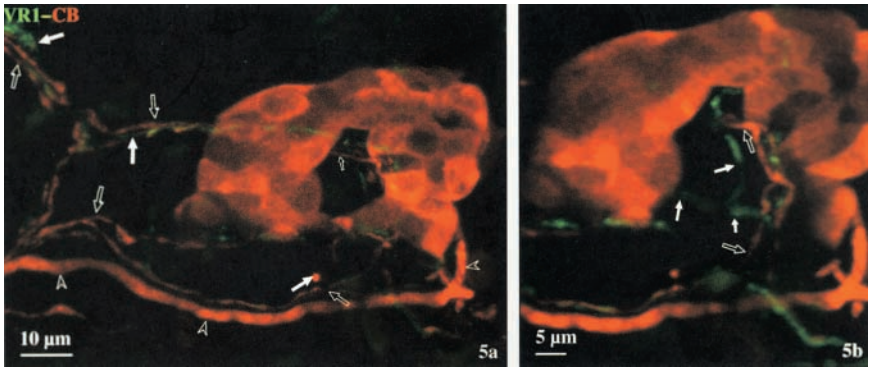

Figure 5. NEB in a respiratory area of the lungs of a 10-d-old rat. (*a*) Maximum intensity projection of 25 confocal optical sections (1-μm interval) of an overview of the innervation pattern of a CB-IR NEB, showing that VR1-IR nerve fibers (*arrows*) do not contain CB, although the thin CB-IR branches (*open arrows*) are seen in very close proximity. Thick CB-IR nerve fibers (*open arrowheads*) can be differentiated more easily. (*b*) High-magnification detail of the basal part of the NEB shown in *a*, revealing in more detail that VR1 IR (*arrows*) and CB IR (*open arrows*) are expressed by different nerve terminals. Maximum intensity projection of five confocal optical sections (1-μm interval).

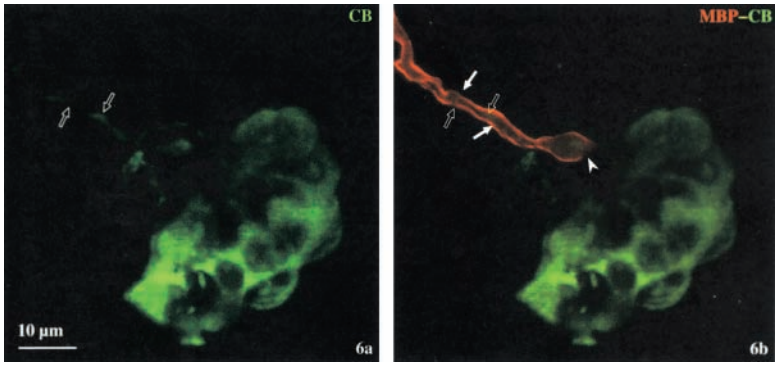

Figure 6. Maximum intensity projection of 23 confocal optical sections (1-µm interval) of a bronchiolar NEB in a 21-d-old rat. TSA-enhanced immunocytochemical staining for CB (*green FITC fluorescence*) and subsequent conventional staining for myelin basic protein (MBP; *red Cy-3 fluorescence*). (*a*) CB-IR NEB contacted by a CB-IR nerve plexus (*open arrows*). (*b*) Combination of the red and green channel shows that the CB-IR nerve fiber (*open arrows*) is surrounded by a MBP-IR myelin sheath (*arrows*), which is lost (*arrowhead*) just before the CB-IR fiber branches and contacts the CB-IR NEB.

demonstrated by their CB (Figure 6) or $P2X_3$ receptor IR (Figure 7), are observed to approach and contact NEBs from PD10 onwards. From PD10 until about postnatal week 5, the number of vagal sensory nerve fibers that becomes myelinated increases. Myelinated vagal sensory nerve fibers can be seen to lose their myelin sheaths in the immediate neighborhood of the target NEBs, after which they branch, and give rise to terminals that penetrate the NEBs (Figures 6 and 7).

Discussion

This study was designed to provide a full functional morphologic characterization of the two clearly distinct sensory nerve fiber populations that selectively contact pulmonary NEBs in rats. The vagal sensory component has its origin in the nodose ganglion, protrudes between the NEB cells, is marked by CB and $P2X_3$ receptor IR, does not express the capsaicin receptor VR1, and is apparently insensitive to systemic capsaicin treatment. Additionally, the vagal nodose sensory

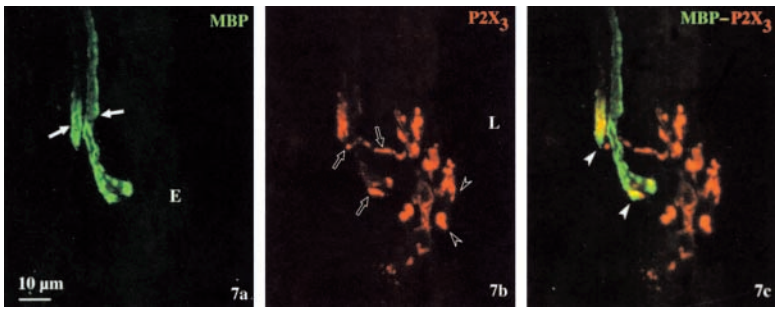

Figure 7. Confocal microscopic images of immunocytochemical double staining for MBP (*green FITC fluorescence*) and $P2X_3$ receptors (*red Cy-3 fluorescence*) in a bronchus of a 21-d-old rat. Maximum intensity projection of 30 optical sections (0.8-µm interval). (*a*) MBP IR can be detected in myelin sheaths (*arrows*) of nerve fibers in close proximity to the bronchial epithelium (E). (*b*) Cy3-labeled nerve fibers expressing $P2X_3$ receptors (*open arrows*) approach the epithelium, branch, protrude between the epithelial cells, and give rise to intraepithelial nerve terminals, many of which (*open arrowheads*) are seen close to the luminal surface (L, lumen of the bronchus). As demonstrated before, such an intraepithelial structure represents an NEB. (*c*) Combination of both channels clearly demonstrates that the $P2X_3$ receptor IR vagal afferent nerve fibers are myelinated. MBP-IR myelin sheaths are lost in close proximity to the target (*arrowheads*).

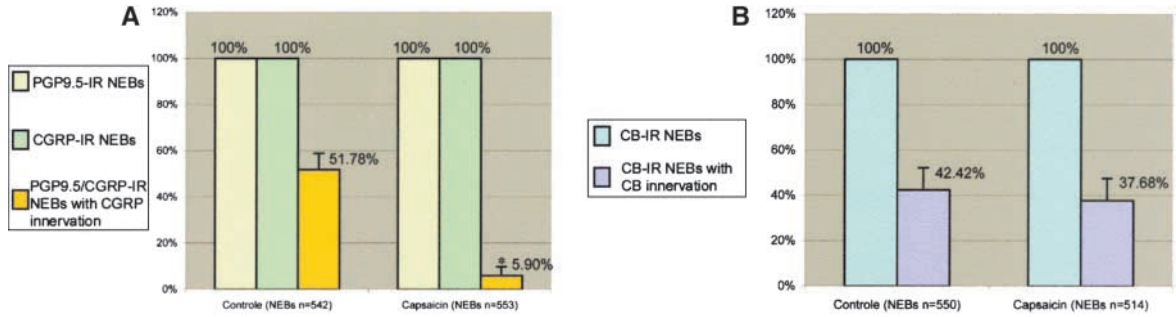

Figure 8. Quantitative analysis of the number of NEBs selectively contacted by spinal (*a*) and vagal (*b*) sensory nerve terminals in capsaicin-treated and nontreated adult rat lungs. Values are mean percentages ± SD of four animals in each group. * $P < 0.05$ versus control rats by Student *t* test. (*a*) Double immunocytochemical staining for PGP9.5 and CGRP clearly shows that after capsaicin treatment, the percentage of NEBs receiving a CGRP-IR innervation is dramatically decreased (*orange bars*). All PGP9.5-IR NEB cells (*yellow bars*), however, showed CGRP IR (*green bars*) in both controls and treated rats, strongly suggesting that capsaicin treatment does not affect the CGRP-content of NEB cells. (*b*) Single staining for CB reveals that capsaicin treatment does not significantly alter the percentage of NEBs contacted by CB-IR nerve terminals.

nerve fiber population innervating NEBs was shown to be myelinated in postnatal lungs. The spinal sensory component of the innervation, on the other hand, is CGRP/SP-IR, contacts only the basal pole of NEBs, expresses VR1, and was additionally proven to be sensitive to systemic capsaicin treatment.

To increase the sensitivity of immunodetection and to allow the consecutive application of two antisera raised in the same species, we visualized some of the antibodies using an amplification method based on the catalyzed deposition of fluorescein- or biotin-conjugated tyramides (20, 22, 23). All controls performed supported the reliability of the labeling using tyramide signal amplification (TSA) in this study. The necessity of more sensitive systems (i.e., biotinylated tyramide amplification) for detection of VR1 (24) and $P2X_3$ receptor IR (15) in peripheral nerve fibers has been reported before.

Previous neuronal tracing experiments (25), and immunocytochemical double labelings using antibodies against CB and the ATP receptor $P2X_3$ (15), already revealed that a subpopulation ($\sim$ 40–45%) of NEBs receives vagal nodose nerve terminals. At the same time, it was clear that intrapulmonary CGRP-IR nerve fibers innervating NEBs always belonged to a sensory nerve fiber population different from the vagal afferent fibers (14, 15). These findings allowed us to use immunocytochemical double staining with antibodies against CB, as a marker for the vagal sensory component, and CGRP, as a marker for the spinal sensory component of the innervation of pulmonary NEBs in rats, in the present study. Subpopulations of NEBs were contacted by thick CB-IR, vagal sensory nerve endings, by thin varicose CGRP-IR nerve terminals or by both nerve fiber populations. In some cases varicose CGRP-IR fibers contacting NEBs showed a very weak CB IR that was not seen before, probably due to the very gentle fixation that was used in combination with a method for optimalization of the tissue for immunostaining (26). Similar co-staining of CGRP and CB in thin varicose spinal afferents has also been reported in rat esophagus (27). In addition, all NEB cells showed IR for both CGRP and CB. Cells that seemed to belong to the organoid NEBs, and expressed CB but no CGRP IR, however, most probably represent Clara-like cells (28), which are known to cover the luminal surface of NEBs.

In the older neuroanatomical literature, some intrapulmonary "sensory" nerve fibers were identified as thick, i.e., myelinated fibers penetrating the airway epithelium and forming complex side branches that terminate in end knobs (29–31). The latter structures were found at widely separate locations, often near airway bifurcations, which is also a preferential location of pulmonary NEBs. An electron microscopic study in rat lungs showed some myelinated nerve fibers that lose their myelin sheaths in close proximity to NEBs (32), but no evidence or suggestion was presented to link these "rare" myelinated fibers to the extensive intraepithelial nerve terminals between NEB cells. The present study confirmed the presence of myelinated nerve fibers that lose their myelin sheaths in the immediate vicinity of NEBs at the light microscopic level and identified them as the extensive vagal nodose component of the selective innervation of pulmonary NEBs. Upon termination of the myelin sheaths, the nerve fibers branched and terminals protruded between the neuroendocrine cells.

The expression of purinergic $P2X_3$ receptors, known as high-threshold receptors (33), on the intraepithelial terminal arborizations of myelinated vagal nodose afferent nerve fibers between pulmonary NEB cells (*see also* Ref. 15) suggests that ATP, secreted by NEB cells, may act as a neurotransmitter/neuromodulator in the vagal sensory transduction of NEBs via a high-threshold $P2X_3$ receptor–mediated fast propagating myelinated pathway. There is increasing evidence that mechanical distortion induces the release of ATP from different cell types (34). The possibility that at least some of the NEBs may act as mechanoreceptors has been suggested before (2, 35), but no direct evidence was presented so far.

Because quinacrine staining showed high levels of ATP in NEBs (15), vagal sensory $P2X_3$ receptor-IR nerve fibers that selectively innervate NEBs may be involved in pulmonary mechanosensory transduction.

For many years, CGRP-IR nerve fibers have been described in very close proximity to or even in contact with pulmonary NEBs (12, 16, 17). However, the intimate relationship between CGRP-IR NEB cells and CGRP-IR nerve fibers, and detailed functional morphological data on the CGRP-IR nerve fiber population selectively innervating NEBs were lacking. Given the well-known co-localization of substance P (SP) and CGRP IR in certain populations of sensory nerve fibers (for rat lungs *see* Ref. 36), we used SP/CGRP double immunolabeling to be able to distinguish the SP/CGRP-IR nerve terminals from the CGRP-IR NEB cells. Unlike the intraepithelially branching vagal sensory terminals, the spinal SP/CGRP-IR endings were mainly located in very close association with the basal pole of pulmonary CGRP-IR NEBs.

Systemic treatment with the vanilloid capsaicin is known to establish a long-lasting depletion of certain populations of afferent nerve fibers (for review *see* Ref. 18), also in rat lungs (16, 17, 36). The present study revealed that in nontreated healthy rat lungs, $\sim$ 50% of the NEBs were contacted by CGRP-IR nerve fibers, whereas 2 wk after systemic capsaicin treatment (125 mg/kg), the subset of NEBs receiving such terminals was decreased to $\sim$ 5%. These results are in agreement with the observations of Shimosegawa and Said (17), who found that the number of CGRP-IR nerve fibers in rat lungs was reduced to almost 0 after neonatal capsaicin treatment (50 mg/kg). The observation that in our study $\sim$ 5% of the NEBs still receives a CGRP-IR innervation, might reflect different morphologic changes induced by capsaicin when given in different doses and at different ages (for review *see* Ref. 18) or a more sensitive detection of CGRP IR in the present study. It has been reported that, with regard to the depletion of peripheral SP/CGRP containing nerve fibers, the subcutaneous administration of 125 mg/kg capsaicin is most effective (37). We are therefore confident that the systemic capsaicin treatment of adult rats in this study induced a selective and effective defunctionalization of capsaicin-sensitive neurons. Further quantitative analysis in the present study revealed that the vagal nodose sensory component of the innervation of pulmonary NEBs, as revealed by CB immunohistochem-

istry, was unaffected in capsaicin-treated rat lungs, because in both control and experimental procedures ~ 40% of the NEBs received a CB-IR innervation.

The actions of capsaicin are mediated through binding with a "capsaicin receptor," VR1, which is a ligand-gated, nonselective cation channel expressed on perikarya and nerve processes of capsaicin-sensitive sensory neurons (24, 38–40). Immunostaining with antibodies against VR1 may therefore be regarded as a marker for capsaicin-sensitive neuronal populations. Using TSA-enhanced immunohistochemical staining for VR1 and subsequent conventional immunolabeling for CGRP, we were able to demonstrate that all spinal CGRP-IR nerve fibers selectively contacting NEBs in rat lungs express VR1, and vice versa. Combination of VR1 and CB immunohistochemistry, on the other hand, revealed that VR1 and CB are not co-expressed in the nodose fibers contacting NEBs, indicating that different nerve fiber populations are concerned. The vagal sensory component of the innervation of NEBs does not express VR1, which explains the apparent insensitivity to capsaicin treatment, which was demonstrated by the comparable percentages of NEBs receiving CB-IR nerve terminals in capsaicin-treated and control rat lungs in the present study.

Other investigators have reported an inconsistent effect of capsaicin treatment on the neuroendocrine cells forming NEBs. It has been suggested that after systemic capsaicin treatment, the CGRP content of pulmonary NEB cells was also depleted (41) or the CGRP IR lowered (16). In our hands, however, all NEBs marked by their PGP9.5 IR showed similar CGRP immunostaining patterns in capsaicin-treated and nontreated rat lungs. Moreover, the lack of VR1 IR on NEB cells strengthens the hypothesis that capsaicin may not be able to exert direct effects on pulmonary neuroendocrine cells. We conclude that capsaicin does not reduce the number of CGRP-IR NEB cells in rat lungs, an assumption also made by Shimosegawa and Said (17).

NEBs represent an extensive local pool of potential vasoactive transmitters such as CGRP (for review *see* Ref. 3). *In vitro* pharmacologic studies have indicated that CGRP exerts a vasodilator effect in rat lungs, and that endogenous CGRP may play an important role in pulmonary pressure homeostasis by directly dilating pulmonary blood vessels (41) via binding to CGRP receptors on vascular smooth muscle (42). Hypoxia apparently inhibits CGRP secretion from rat NEBs (43), and local physiologic hypoxia may therefore result in local vasoconstriction. It has been found that intact primary sensory CGRP/SP-containing and capsaicin-sensitive nerve fibers are required for endogenous CGRP to modulate pulmonary vascular tone in hypoxic pulmonary hypertension (41). In a recent investigation we provided morphologic evidence that all NEBs receiving an intraepithelial nitrergic innervation also revealed basal contacts with CGRP-IR afferents, the presumable collaterals of which appear to follow the course of nitrergic axons and eventually form baskets around the nitrergic neurons in the lamina propria (21). It was proposed that hypoxia may reduce CGRP secretion from NEB cells via a nitrergic mechanism, the activation of which involves the presently characterized population of capsaicin-sensitive CGRP-IR afferents that selectively contact NEBs, thereby resulting in a normal adaptation of local blood flow to the aeration in different areas of the lungs (21).

Recently, Widdicombe (1) reviewed the classification of pulmonary afferent receptors. Most physiologic studies, however, disclose little or no data about the morphology of, and the intimate relationship between, airway receptor terminals and the tissue environment, which is important information for understanding the mechanisms of transduction of physical, chemical, or other stimuli in neuronal activity. In the present study, we provided evidence that NEBs in rat lungs receive a dual sensory innervation, and evaluated the typical properties reported for physiologically "characterized" airway receptors. The fine varicose unmyelinated, capsaicin-sensitive, CGRP/SP/VR1-IR nerve fibers, selectively contacting the base of part of the pulmonary NEBs, revealed typical C-fiber characteristics but, at least for the largest part, do not have the vagal sensory origin that was reported for bronchopulmonary C-fiber receptors. The myelinated, capsaicin-insensitive, CB- and $P2X_3$ receptor-IR nerve endings contacting NEBs, on the other hand, are known to have a vagal origin. In the past, suggestions have been made to correlate pulmonary NEBs to physiologically characterized counterparts such as irritant receptors (RARs) (44). However, there are no claims for recordings from single vagal afferent fibers from NEBs, and in general all recordings of the effect of airway hypoxia in vagal afferent fibers have yielded negative results (1); SARs, RARs, and C-fiber receptors are apparently not directly affected by hypoxia in physiologic experiments (45). Among the types of vagal receptors reported in lower airways so far, SARs and RARs appear to be connected to myelinated afferent nerves, the latter to thin, so-called Aδ fibers. Based on poor morphologic evidence, the terminals of SARs are considered by lung physiologists to be located in airway smooth muscle. Experimental evidence suggests that RARs are, at least partly, represented by intraepithelial terminals, but are mainly located in extrapulmonary airways, are scanty in smaller bronchi, and are absent in bronchioles and respiratory areas (1). According to these criteria, the population of myelinated vagal afferent fibers that gives rise to selective intraepithelial terminals in NEBs at all levels of the airways apparently does not fit into one of the so far characterized types of myelinated lung receptors. It seems, however, very unlikely that lung physiologists, performing many thousands of single fiber recordings in the vagus nerve for the identification of airway receptor populations in rat lungs, have never made registrations from the many hundreds of myelinated vagal nodose neurons that selectively contact pulmonary NEBs in each lung. More likely, the population(s) concerned ha(s)(ve) so far not been recognized in the existing data. Therefore, we believe that a considerable part of the already "characterized" airway receptors, a large part of which are mechanoreceptors, will eventually appear to be related to NEBs.

Also in the gut wall it has been suggested that electrophysiologic and morphologic analyses of vagal mechanoreceptors give rise to conflicting interpretations (46). Although electrophysiology distinguished a single general class of endings in smooth muscle, morphology provided evidence that besides very few intramuscular endings, a large

pool of potential mechanoreceptor endings, the so-called intraganglionic laminar endings, were present in myenteric ganglia located between the muscle layers of the muscularis propria of the gut wall (46, 47). Immunostaining of rat esophagus, especially for calcium-binding proteins, provided evidence that vagal afferents mainly give rise to intraganglionic laminar endings, and to mucosal end organs (27, 48, 49) similar to those found in the laryngeal (50), tracheal, and bronchial mucosa of the rat (51).

In contrast to the multiplicity of airway receptors, apparently monitoring mucosal events, that were identified by physiologists, descriptions of morphologically well-characterized airway receptor terminals are rare. This implicates that most mucosal pulmonary receptors have a poorly identified morphology, or that a more complex receptor "organ" is able to integrate various sensory activities. NEBs are clearly the most eye-catching intraepithelial receptors in the lung. Although surely not all components of the extremely complex innervation of pulmonary NEBs in rats have been fully characterized at present, it is quite clear that the pattern is not identical for all NEBs. However, because the role of any NEB nerves is still largely a matter of speculation, it would be premature to divide the population of pulmonary NEBs into subgroups, based on these innervation patterns only. Although the physiologic significance of the complex innervation pattern of pulmonary NEBs is still mysterious, the sensory nature of NEBs seems beyond dispute. The present data suggest that pulmonary NEBs represent an extensive population of complex intraepithelial receptors that may be able to accommodate various chemo- and mechanosensory modalities.

Acknowledgments: This study was supported by an IWT (SB 981363 to I.B.) and an FWO grant (G.0155.01 to D.W.S.) from the Flemish Government, and by a NOI-BOF grant from the University of Antwerp. The authors wish to thank H. De Pauw, D. De Rijck, R. Spillemaeckers, G. Svensson, F. Terloo, J. Van Daele, G. Vermeiren, and D. Vindevogel for excellent assistance during the preparation of this work.

References

1. Widdicombe, J. G. 2001. Airway receptors. *Respir. Physiol.* 125:3–15.
2. Lauweryns, J. M., M. Cokelaere, and P. Theunynck. 1972. Neuroepithelial bodies in the respiratory mucosa of various mammals: a light optical, histochemical and ultrastuctural investigation. *Z. Zellforsch. Mikrosk. Anat.* 135:569–592.
3. Adriaensen, D., and D. W. Scheuermann. 1993. Neuroendocrine cells and nerves of the lung. *Anat. Rec.* 236:70–85.
4. Sorokin, S. P., and R. F. Hoyt. 1989. Neuroepithelial bodies and solitary small-granule cells. *In* Lung Cell Biology. D. Massaro, editor. Marcel Dekker, New York. 191–344.
5. Youngson, C. R., C. Nurse, H. Yeger, J. T. Curnutte, C. Vollmer, V. Wong, and E. Cutz. 1997. Immunocytochemical localization on O_2-sensing protein (NADPH oxidase) in chemoreceptor cells. *Microsc. Res. Tech.* 37: 101–106.
6. Youngson, C., C. Nurse, H. Yeger, and E. Cutz. 1993. Oxygen sensing in airway chemoreceptors. *Nature* 365:153–155.
7. O'Kelly, I., A. Lewis, C. Peers, and P. J. Kemp. 2000. O_2 sensing by airway chemereceptor-derived cells. Protein kinase C activation reveals functional evidence for involvement of NADPH oxidase. *J. Biol. Chem.* 275: 7684–7692.
8. Fu, X. W., C. A. Nurse, V. Wong, and E. Cutz. 2002. Hypoxia-induced secretion of serotonin from intact pulmonary neuroepithelial bodies in neonatal rabbit. *J. Physiol.* 539:503–510.
9. Hartness, M. E., A. Lewis, G. J. Searle, I. O'Kelly, C. Peers, and P. J. Kemp. 2001. Combined antisense and pharmacological approaches implicate hTASK as an airway O_2 sensing K^+ channel. *J. Biol. Chem.* 276:26499–26508.
10. Cutz, E., and A. Jackson. 1999. Neuroepithelial bodies as airway oxygen sensors. *Respir. Physiol.* 115:201–214.
11. Peers, C., and P. J. Kemp. 2001. Acute oxygen sensing: diverse but convergent mechanisms in airway and arterial chemoreceptors. *Respir. Res.* 2:145–149.
12. Sorokin, S. P., R. F. Hoyt, and M. J. Shaffer. 1997. Ontogeny of neuroepithelial bodies: correlations with mitogenesis and innervation. *Microsc. Res. Tech.* 37:43–61.
13. Sorokin, S. P., and R. F. Hoyt. 1990. On the supposed function of neuroepithelial bodies in adult mammalian lungs. *News Physiol. Sci.* 5:89–95.
14. Adriaensen, D., J.-P. Timmermans, I. Brouns, H.-R. Berthoud, W. L. Neuhuber, and D. W. Scheuermann. 1998. Pulmonary intraepithelial vagal nodose afferent nerve terminals are confined to neuroepithelial bodies: an anterograde tracing and confocal microscopy study in adult rats. *Cell Tissue Res.* 293:395–405.
15. Brouns, I., D. Adriaensen, G. Burnstock, and J.-P. Timmermans. 2000. Intraepithelial vagal sensory nerve terminals in rat pulmonary neuroepithelial bodies express $P2X_3$ receptors. *Am. J. Respir. Cell Mol. Biol.* 23:52–61.
16. Cadieux, A., D. R. Springall, P. K. Mulderry, J. Rodrigo, M. A. Ghatei, G. Terenghi, S. R. Bloom, and J. M. Polak. 1986. Occurrence, distribution and ontogeny of CGRP immunoreactivity in the rat lower respiratory tract: effect of capsaicin treatment and surgical denervations. *Neuroscience* 19:605–627.
17. Shimosegawa, T., and S. I. Said. 1991. Pulmonary calcitonin gene-related peptide immunoreactivity: nerve-endocrine cell interrelationships. *Am. J. Respir. Cell Mol. Biol.* 4:126–134.
18. Holzer, P. 1991. Capsaicin: cellular targets, mechanisms of action, and selectivity for thin sensory neurons. *Pharmacol. Rev.* 43:143–201.
19. Garbay, B., A. M. Heape, F. Sargueil, and C. Cassagne. 2000. Myelin synthesis in the peripheral nervous system. *Prog. Neurobiol.* 61:267–304.
20. Brouns, I., L. Van Nassauw, J. Van Genechten, M. Majewski, D. W. Scheuermann, J.-P. Timmermans, and D. Adriaensen. 2002. Triple immunofluorescence staining method with antibodies raised in the same species to study the complex innervation pattern of intrapulmonary chemoreceptors. *J. Histochem. Cytochem.* 50:575–582.
21. Brouns, I., J. Van Genechten, D. W. Scheuermann, J.-P. Timmermans, and D. Adriaensen. 2002. Neuroepithelial bodies: a morphological substrate for the link between neuronal nitric oxide and sensitivity to airway hypoxia? *J. Comp. Neurol.* 449:343–354.
22. Hunyady, B., K. Krempels, G. Harta, and E. Mezey. 1996. Immunohistochemical signal amplification by catalyzed reporter deposition and its application in double immunostaining. *J. Histochem. Cytochem.* 44:1353–1362.
23. Shindler, K. S., and K. A. Roth. 1996. Double immunofluorescent staining using two unconjugated primary antisera raised in the same species. *J. Histochem. Cytochem.* 44:1331–1335.
24. Guo, A., L. Vulchanova, J. Wang, X. Li, and R. Elde. 1999. Immunocytochemical localisation of the vanilloid receptor 1 (VR1): relationship to neuropeptides, the $P2X_3$ purinoceptor and IB4 binding sites. *Eur. J. Neurosci.* 11:946–958.
25. Adriaensen, D., J.-P. Timmermans, I. Brouns, H.-R. Berthoud, W. L. Neuhuber, and D. W. Scheuermann. 1998. Pulmonary intraepithelial vagal nodose afferent nerve terminals are confined to neuroepithelial bodies: an anterograde tracing and confocal microscopy study in adult rats. *Cell Tissue Res.* 293:395–405.
26. Llewellyn-Smith, I. J., M. Costa, and J. B. Furness. 1985. Light and electron microscopic immunocytochemistry of the same nerves from whole mount preparations. *J. Histochem. Cytochem.* 33:857–866.
27. Dütsch, M., U. Eichhorn, J. Wörl, M. Wank, H.-R. Berthoud, and W. L. Neuhuber. 1998. Vagal and spinal afferent innervation of the rat esophagus: a combined retrograde tracing and immunocytochemical study with special emphasis on calcium-binding proteins. *J. Comp. Neurol.* 398: 289–307.
28. Adriaensen, D., D. W. Scheuermann, M. Gajda, I. Brouns, and J.-P. Timmermans. 2001. Functional implications of extensive new data on the innervation of pulmonary neuroepithelial bodies. *Ital. J. Anat. Embryol.* 106:395–405.
29. Larsell, O. 1921. Nerve termination in the lung of the rabbit. *J. Comp. Neurol.* 33:105–132.
30. Larsell, O., and R. S. Dow. 1933. The innervation of the human lung. *Am. J. Anat.* 52:125–146.
31. Spencer, H., and D. Leof. 1964. The innervation of human lung. *J. Anat.* 98:599–609.
32. Van Lommel, A., and J. M. Lauweryns. 1993. Neuroepithelial bodies in the Fawn Hooded rat lung: morphological and neuroanatomical evidence for a sensory innervation. *J. Anat.* 183:553–566.
33. Cook, S. P., L. Vulchanova, K. M. Hargreaves, R. Elde, and E. W. McCleskey. 1997. Distinct ATP receptors on pain-sensing and stretch-sensing neurons. *Nature* 387:505–508.
34. Burnstock, G. 1999. Release of vasoactive substances from endothelial cells by shear stress and purinergic mechano-sensory transduction. *J. Anat.* 194:335–343.
35. Wasano, K., and T. Yamamoto. 1978. Monoamine-containing granulated cells in the frog lung. *Cell Tissue Res.* 193:201–209.
36. Martling, C.-R., A. Saria, A. Fischer, T. Hokfelt, and J. M. Lundberg. 1988. Calcitonin gene-related peptide and the lung: neuronal coexistence with

substance P, release by capsaicin and vasodilatory effect. *Regul. Pept.* 20: 125–139.
37. Gamse, R., S. E. Leeman, P. Holzer, and F. Lembeck. 1981. Differential effects of capsaicin pretreatment on the content of somatostatin, substance P, and neurotensin in the nervous system of the rat. *Naunyn Schmiedebergs Arch. Pharmacol.* 317:140–148.
38. Caterina, M. J., M. A. Schumacher, M. Tominaga, T. A. Rosen, J. D. Levine, and D. Julius. 1997. The capsaicin receptor: a heat-activated ion channel in the pain pathway. *Nature* 389:816–824.
39. Szallasi, A., and P. M. Blumberg. 1999. Vanilloid (Capsaicin) receptors and mechanisms. *Pharmacol. Rev.* 51:159–211.
40. Tominaga, M., M. J. Caterina, A. B. Malmberg, T. A. Rosen, H. Gilbert, K. Skinner, B. E. Raumann, A. I. Basbaum, and D. Julius. 1998. The cloned capsaicin receptor integrates multiple pain-producing stimuli. *Neuron* 21:531–543.
41. Tjen-A-Looi, S., H. Kraiczi, R. Ekman, and I. M. Keith. 1998. Sensory CGRP depletion by capsaicin exacerbates hypoxia-induced pulmonary hypertension in rats. *Regul. Pept.* 74:1–10.
42. Qing, X., J. Svaren, and I. M. Keith. 2001. mRNA expression of novel CGRP1 receptors and their activity modifying proteins in hypoxic rat lung. *Am. J. Physiol. Lung Cell. Mol. Physiol.* 280:L547–L554.
43. Springall, D. R., and J. M. Polak. 1993. Calcitonin gene-related peptide and pulmonary hypertension in experimental hypoxia. *Anat. Rec.* 236:96–104.
44. Van Lommel, A., J. M. Lauweryns, and H.-R. Berthoud. 1998. Pulmonary neuroepithelial bodies are innervated by vagal afferent nerves: an investigation with *in vivo* anterograde DiI tracing and confocal microscopy. *Anat. Embryol.* 197:325–330.
45. Coleridge, H. M., and J. C. Coleridge. 1997. Afferent nerves in the airways. *In* Autonomic Control of the Respiratory System. P. J. Barnes, editor. Taylor & Francis, London. 39–58.
46. Phillips, R. J., and T. L. Powley. 2000. Tension and stretch receptors in gastrointestinal smooth muscle: re-evaluating vagal mechanoreceptor physiology. *Brain Res. Brain Res. Rev.* 34:1–26.
47. Neuhuber, W. L., M. Kressel, A. Stark, and H.-R. Berthoud. 1998. Vagal efferent and afferent innervation of the rat esophagus as demonstrated by anterograde DiI and DiA tracing: focus on myenteric ganglia. *J. Auton. Nerv. Syst.* 70:92–102.
48. Kuramoto, H., and R. Kuwano. 1994. Immunohistochemical demonstration of calbindin-containing nerve endings in the rat esophagus. *Cell Tissue Res.* 278:57–64.
49. Wank, M., and W. L. Neuhuber. 2001. Local differences in vagal afferent innervation of the rat esophagus are reflected by neurochemical differences at the level of the sensory ganglia and by different brainstem projections. *J. Comp. Neurol.* 435:41–59.
50. Yamamoto, Y., Y. Atoji, H. Kuramoto, and Y. Suzuki. 1998. Calretinin-immunoreactive laminar nerve endings in the laryngeal mucosa of the rat. *Cell Tissue Res.* 292:613–617.
51. Yamamoto, Y., Y. Atoji, and Y. Suzuki. 1999. Calretinin immunoreactive nerve endings in the trachea and bronchi of the rat. *J. Vet. Med. Sci.* 61: 267–269.